Replica theory for fluctuations of the activation barriers in glassy systems

Maxim Dzero,[1] Jörg Schmalian,[2] and Peter G. Wolynes[3]
[1]*Center for Materials Theory, Rutgers University, Piscataway, New Jersey 08854, USA*
[2]*Department of Physics and Astronomy and Ames Laboratory, Iowa State University, Ames, Iowa 50011, USA*
[3]*Department of Chemistry and Biochemistry and Department of Physics, University of California, San Diego, La Jolla, California 92093, USA*
(Received 3 October 2008; revised manuscript received 5 May 2009; published 16 July 2009)

We consider the problem of slow activation dynamics in glassy systems undergoing a random first-order phase transition. Using an effective potential approach to supercooled liquids, we determine the spectrum of activation barriers for entropic droplets. We demonstrate that fluctuations of the configurational entropy and of the liquid glass surface tension are crucial to achieve an understanding of the barrier fluctuations in glassy systems and thus are ultimately responsible for the broad spectrum of excitations and heterogeneous dynamics in glasses. In particular we derive a relation between the length scale for dynamic heterogeneity and the related barrier fluctuations. Diluted entropic droplets are shown to have a Gaussian distribution of barriers, strongly suggesting that non-Gaussian behavior results from droplet-droplet interactions.

DOI: 10.1103/PhysRevB.80.024204 PACS number(s): 75.10.Nr, 05.70.Ln

I. INTRODUCTION

The glass transition and glassy behavior are dynamical phenomena characterized by slow relaxations and a broad spectrum of excitations. Recently strong experimental evidence for dynamical heterogeneity in glassy systems, i.e., for spatially varying characteristic time scales for relaxation, has been obtained through NMR (Ref. 1) and nanometer-scale probing of dielectric fluctuations.[2] The wide distribution of excitations, as seen in bulk dielectric measurements, is therefore believed to be caused largely by spatial variation in the characteristic time scales; see also Ref. 3. Regions in a glassy system separated by only a few nanometers relax on time scales different by many orders of magnitude.

Whether these purely dynamical phenomena can be explained in terms of the underlying *energy landscape* is still debated. The question has been positively answered on the level of the mean-field theory of glasses. The dynamical, ideal mode-coupling theory[4] and energy landscape based replica mean-field theories were demonstrated to describe the same underlying physics yet from rather different perspectives.[5,6] The idealized version of the mode-coupling theory[4] falls out of equilibrium below a temperature $T_A > T_g$, where T_g is the laboratory glass temperature (see below). This is consistent with static energy landscape based mean-field theories that find the emergence of exponentially many metastable states, $\mathcal{N}_{\rm ms} \propto \exp(\text{const.}V)$, at the same temperature T_A. Here V is the volume of the system. Thus, the configurational entropy $S_c = k_B \log \mathcal{N}_{\rm ms}$ becomes extensive and only vanishes at the Kauzmann temperature $T_K < T_A$. Unfortunately, neither the emergence of slow activated dynamics nor the possibility of spatial heterogeneity is correctly captured within mean-field theory, making it impossible to use mean-field theory alone to directly explain the heterogeneous dynamics observed in numerous glass-forming liquids. On the other hand, mode-coupling theory at higher temperatures ($T > T_A$) has been shown to give a reasonably accurate account of the dynamics of liquids. At lower temperatures ($T < T_A$), bulk thermodynamic properties of glass-forming liquids, most notably the temperature dependence of the configurational entropy and the related Kauzmann paradox,[7] agree with the results of the energy landscape based mean-field theory (see Refs. 8 and 9). This motivated the development of a theory for glass-forming liquids that has its foundation in the mean-field theory, but that does take into account activated dynamics and spatial heterogeneity which are beyond the strict mean-field approach.[5,8] The resulting random first-order (RFOT) theory of glasses demonstrates that ergodicity above the Kauzmann temperature T_K can be restored via "entropic droplets" in which a region of the liquid is replaced by any of an exponentially large number of alternatives. The entropy of the possible alternatives acts as a driving force for structure change. This driving force is offset by the free-energy cost of matching two alternative structures at their boundaries. This conflict gives a free-energy barrier for activated motions.[5,10] Various consequences of entropic droplets have been analyzed in Refs. 11–14 using for concrete calculation a density functional description of the liquid state. These quantitative results have been found to be in good agreement with experiment. Within RFOT, the number of metastable states determines the activation barrier of the glassy state. While this is similar to the Adam-Gibbs theory for glasses,[15] there exist important distinctions between the two approaches (see Ref. 10). In agreement with the RFOT approach but not with the assumptions of Adam-Gibbs argument, the complexity of a correlated region increases as the glass transition is approached.[16] The need for instantonlike events to understand the longtime dynamics in glasses is also supported by recent findings on extended mode-coupling theories for dense fluids.[17]

More recently, an effective Landau theory for glasses, based on the replica method of Ref. 18, has been developed. This framework naturally allows for activated dynamics beyond mean-field theory.[19,20] This approach based on instantons offers a formal justification of the entropic droplet approach using the replica approach to glasses. It reproduces and thus confirms several results of the RFOT theory of structural glasses.[8] In both approaches, a mean droplet acti-

vation energy $\overline{F^{\ddagger}}$ occurs, which is determined by the configurational entropy density s_c (for details see below),

$$\overline{F^{\ddagger}} \propto s_c^{1-d\nu}. \tag{1}$$

$s_c \propto \frac{T-T_K}{T_K}$ vanishes linearly at the Kauzmann temperature $T_K < T_g$. The exponent ν relates the droplet size R and the configurational entropy density: $R \propto s_c^{-\nu}$. d is the spatial dimension. Below we assume that $d=3$. In its most elementary version the replica Landau theory yields $\nu=1$.[19,20] A renormalization of the droplet interface due to wetting of intermediate states on the droplet surface[8] was shown to yield $\nu = 2/d$, leading to $\overline{F^{\ddagger}} \propto T s_c^{-1}$ and correspondingly to a Vogel-Fulcher law $\bar{\tau} \simeq \tau_0 \exp(\frac{DT_K}{T-T_K})$ for the mean relaxation time,

$$\bar{\tau} = \tau_0 \exp\left(\frac{\overline{F^{\ddagger}}}{k_B T}\right). \tag{2}$$

A softening of the surface tension due to replica symmetry breaking of the instanton solution was also obtained in Ref. 20 and seems to be a first correction containing the effects that lead to a reduction in the exponent ν from the value of $\nu=1$.

Numerous experiments on supercooled liquids not only depend on the most probable barrier, $\overline{F^{\ddagger}}$, but are also sensitive to the entire broad excitation spectrum in glasses.[3] Most notably, the broad peaks in the imaginary part of the dielectric function $\varepsilon''(\omega)$ are most naturally understood in terms of a distribution $g(\tau)$ of relaxation times such that

$$\varepsilon''(\omega) \propto \int d\tau g(\tau) \frac{\omega\tau}{1+(\omega\tau)^2}. \tag{3}$$

Similarly dynamical heterogeneity with spatially fluctuating relaxation times yields nonexponential (frequently stretched exponential) relaxation of the correlation function,

$$\phi(t) = \int d\tau g(\tau) e^{-t/\tau}, \tag{4}$$

and allow for an explanation of nonresonant hole burning experiments[21] even though interesting interpretations of the nonexponentiality based on "dynamical homogeneity" exist as well.[22] Other effects that are most likely caused by a distribution of relaxation rates include the breakdown of the Stokes-Einstein relation $D=\frac{k_B T}{4\pi\eta L}$ between the diffusion coefficient D of a particle of size L and the viscosity η.[23,24]

These experiments all call for a more detailed analysis of the fluctuations,

$$\overline{\delta F^{\ddagger 2}} \equiv \overline{F^{\ddagger 2}} - \overline{F^{\ddagger}}^2,$$

of the activation barriers and, more generally, of the distribution function $p(F^{\ddagger})$ of barriers. The latter yields the distribution function of the relaxation times,

$$g(\tau) = p(F^{\ddagger}) \frac{dF^{\ddagger}}{d\tau}, \tag{5}$$

through $\tau(F^{\ddagger}) = \tau_0 \exp(\frac{F^{\ddagger}}{k_B T})$. For example, in case of a Gaussian distribution of barriers one obtains a broad log-normal distribution of relaxation rates,

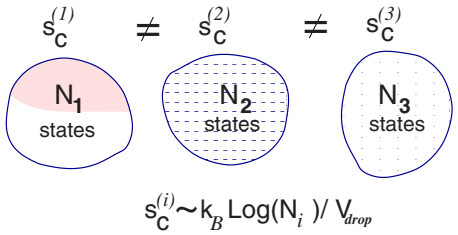

FIG. 1. (Color online) The appearance of an exponentially large number of metastable configurations and the possibility for a system to realize these configurations give rise to the configurational entropy. The latter serves as the driving force for the structure change in the glassy phase. The energy cost to match the boundaries between the different density configurations gives rise to the energy barriers. The fluctuations of the configurational entropy give rise to the energy barrier fluctuations.

$$g(\tau) = \frac{1}{\tau\sqrt{2\pi\lambda}} \exp\left(-\frac{\log^2(\tau/\bar{\tau})}{2\lambda}\right), \tag{6}$$

with

$$\lambda = \overline{\delta F^{\ddagger 2}}/(k_B T)^2 \tag{7}$$

and $\bar{\tau}$ from Eq. (2). While the distribution [Eq. (6)] does not yield precisely a stretched exponential form for the correlation function, it can often be approximated by

$$\phi(t) \simeq \exp(-(t/\bar{\tau})^{\beta}), \tag{8}$$

with $\beta=(1+\lambda)^{-1/2}$. Furthermore, the study of higher order moments of $p(F^{\ddagger})$ is important to determine whether the distribution is indeed Gaussian or more complicated.

In this paper we determine the fluctuations $\overline{\delta F^{\ddagger 2}}$ as well as higher moments of the distribution of the barrier distribution function $p(F^{\ddagger})$. Thus, we address the following question: what are the fluctuations of this optimal barrier around its most probable value? Due to the distribution of metastable states the barrier is sometimes a little larger and is sometimes a bit smaller. Our theory gives a quantitative answer as to how much larger and smaller. We start from the replica Landau theory of Ref. 18 and use the replica instanton theory of Refs. 19 and 20. We then generalize the replica formalism to determine barrier fluctuations in addition to the determination of the mean barrier $\overline{F^{\ddagger}}$. Our approach is an important step to gain insight into the whole spectrum of activated processes in glassy systems in general.

The role of barrier fluctuations within the RFOT theory of structural glasses was first discussed by Xia and Wolynes in Ref. 12. Variations in the configurational entropy density were assumed to be the main cause of the fluctuations of the barrier (Fig. 1).

Starting from $F^{\ddagger} \propto s_c^{1-d\nu}$, barrier and configurational entropy density fluctuations are related by $\delta F^{\ddagger} \propto s_c^{-d\nu} \delta s_c$, which yields $\overline{\delta F^{\ddagger 2}} \propto s_c^{-2d\nu} \overline{\delta s_c^2}$. Standard fluctuation theory then determines the entropy fluctuations in a region of size R^d as $\overline{\delta s_c^2} \propto \Delta c_p R^{-d}$ where the configurational heat capacity remains finite as $T \to T_K$ (for a detailed discussion of Δc_p see below). This reasoning finally yields

$$\overline{\delta F^{\ddagger 2}} \propto s_c^{-d\nu} \propto R^d. \tag{9}$$

In the approach of Ref. 12, barrier fluctuations diverge with the volume of the entropic droplet. Our results will demonstrate that the leading droplet size dependence of $\overline{\delta F^{\ddagger 2}}$ agrees with Eq. (9) and Ref. 12. We also show that there are additional terms originating in the fluctuations of the interface tension of entropic droplets that contribute to $\overline{\delta F^{\ddagger 2}}$. In addition we analyze the temperature dependence of the static barrier fluctuations and of the exponent β for stretched exponential relaxation as well as the variation in the dielectric response with frequency and temperature.

We stress that there may, in principle, be experiments that probe certain dynamical processes that deviate from the most probable barrier in ways that differ from our procedure. These could result in tails in the distribution of relaxation times. Indeed, a pileup of short, not long, relaxation times is observed and is called beta relaxation. We believe that these beta relaxations occur via transition states that deviate considerably in shape from the most probable one. Notice however that they have small effect on the moment of the barriers that occur on the low barrier side of the distribution. To determine these, another calculation is needed since our theory does not apply in that case.

This paper is organized as follows. In the next section we introduce the replica effective potential formalism to analyze barrier fluctuations in glass-forming liquids. We motivate the approach by starting from a density functional approach to liquids and by using an equilibrium replica theory to derive the mean-field theory as the starting point of our calculation. Next we analyze fluctuations of the configurational entropy in bulk; summarize the effective potential approach of Ref. 18 and the instanton calculation that yields the most probable barrier $\overline{F^{\ddagger}}$. Finally we demonstrate how higher moments of the barrier distribution can be derived within the same formalism. At the end of the section we present our results for physical observables. The paper is concluded with a summarizing section.

II. REPLICA EFFECTIVE POTENTIAL FORMALISM

A. Motivation and cloned replica approach

We start our description of glassy systems from the point of view that there exists a density functional, $\phi[\rho]$, that describes a supercooled liquid undergoing a mean-field glass transition. Initially, such an approach was used in Ref. 25 where it was shown that it allows one to describe the emergence of a metastable amorphous solid (Fig. 2). Following the classical approach to freezing into ordered crystalline states,[26] the density was assumed to be $\rho(\mathbf{r}) = (\frac{\alpha}{\pi})^{3/2} \Sigma_i e^{-\alpha(\mathbf{r}-\mathbf{r}_i)^2}$. Here, α determines the Lindemann length, $\alpha^{-1/2}$ over which particles are localized. In distinction to crystallization, the mean positions, $\mathbf{r}_i$, of an amorphous solid were taken to be those of a random hard sphere packing[27] instead of the periodic crystal lattice positions. The free energy of this amorphous solid was shown to have a global minimum at $\alpha=0$ and a local minimum for finite α. If $\alpha \simeq V^{-2/3} \to 0$, the particles are delocalized and the system in an ergodic liquid state with homogeneous density $\rho_0 = \frac{N}{V}$. Finite α corresponds to a frozen amorphous solid, i.e., a glassy state. For $T > T_K$ the amorphous solid is metastable with respect to the liquid and is higher in free energy by TS_c. It is of course always metastable with respect to the crystalline solid.

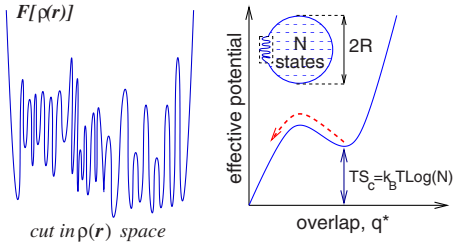

FIG. 2. (Color online) The typical energy landscape in the structural glassy phase as a function of density (left panel) and the effective potential, which is used to describe the transition between the nonergodic glassy states and the ergodic liquid state (right panel).

Essentially the same mean-field physics can be described in terms of a formally more precise replica approach, introduced by Monasson.[28] Here one determines the partition function in the presence of a bias configuration $\hat{\rho}(r)$,

$$Z[\hat{\rho}] = \int D\rho e^{-\beta\phi[\rho] - g\int d^d x[\rho(x) - \hat{\rho}(x)]^2}. \tag{10}$$

Here, $\int D\rho \cdots$ corresponds to the statistical sum over all density configurations of the system. The free energy of a bias configuration is

$$f[\hat{\rho}] = -T \log Z[\hat{\rho}]. \tag{11}$$

Physically $f[\hat{\rho}]$ can be interpreted as the free energy for a metastable amorphous configuration of atoms, for example, with density $\hat{\rho}(x)$ being a sum over Gaussians discussed above. In the replica formalism, no specific configuration such as this needs to be specified in order to perform the calculation. Rather, the assumption is made that the probability distribution for metastable configurations is determined by $f[\hat{\rho}]$ accordingly,

$$P[\hat{\rho}] \propto \exp(-\beta_{\text{eff}} f[\hat{\rho}]), \tag{12}$$

and is characterized by the effective temperature $T_{\text{eff}} = \beta_{\text{eff}}^{-1} \geq T$. This allows one to determine the mean free energy,

$$\bar{F} = \int D\hat{\rho} f[\hat{\rho}] P[\hat{\rho}], \tag{13}$$

and the corresponding mean configurational entropy,

$$\overline{S_c} = -\int D\hat{\rho} P[\hat{\rho}] \log P[\hat{\rho}]. \tag{14}$$

The approach of Ref. 28 was successfully used to develop a mean-field theory for glass formation in supercooled liquids[29] yielding results in detailed agreement with earlier nonreplica approaches.[30] As shown by Monasson,[28] the mean values $\bar{F}$ and $\overline{S_c}$ can be determined from a replicated partition function,

$$Z[m] = \int D^m \rho e^{-\beta \Sigma_{a=1}^m \phi[\rho_a] + g \Sigma_{a,b=1}^m \int d^d x \rho_a(x) \rho_b(x)}, \quad (15)$$

via $\bar{F} = \frac{\partial}{\partial m} m F(m)$ and $\overline{S_c} = \frac{m^2}{T} \frac{\partial}{\partial m} F(m)$ with

$$F(m) = -\frac{T}{m} \log Z(m) \quad (16)$$

and replica index $m = \frac{T}{T_{\text{eff}}}$. It follows from the replicated free energy $F(T_{\text{eff}})$ that

$$\bar{F} = -T_{\text{eff}}^2 \frac{\partial [F(T_{\text{eff}})/T_{\text{eff}}]}{\partial T_{\text{eff}}},$$

$$\overline{S_c} = -\frac{\partial F(T_{\text{eff}})}{\partial T_{\text{eff}}}. \quad (17)$$

These results are in analogy to the usual thermodynamic relations among free energy $[F \to F(T_{\text{eff}})]$, internal energy $(U \to \bar{F})$, entropy $(S \to \overline{S_c})$, and temperature $(T \to T_{\text{eff}})$ (see also Ref. 31). If the liquid gets frozen in one of the many metastable states, the system cannot anymore realize its configurational entropy; i.e., the mean free energy of frozen states is $\bar{F}$, higher by $T\overline{S_c}$ if compared to the equilibrium free energy of the liquid, Fig. 2.

If the replica solution is taken to be marginally stable so that the lowest eigenvalue of the fluctuation spectrum beyond mean-field solution vanishes, it has been shown[32] that T_{eff} agrees with the result obtained from the generalized fluctuation-dissipation theorem in the dynamic description of mean-field glasses.[33] Typically, the assumption of marginality is appropriate for early times right after a rapid quench from high temperatures. In this case $T_{\text{eff}} > T$ for $T < T_A$; i.e., the distribution function of the metastable states is not in equilibrium on the time scales where mode-coupling theory or the requirement for marginal stability applies. Above the Kauzmann temperature it is however possible also to consider the solution where $T_{\text{eff}} = T$, i.e., where the distribution of metastable states has equilibrated with the external heat bath of the system. Since we are interested in a system where ergodicity is restored for $T_K < T < T_A$ we use $T_{\text{eff}} = T$. Technically this is a supercooled liquid and not a nonequilibrium aging glass. Below the Kauzmann temperature this assumption cannot be made any longer (at least within the mean-field theory) as it leads to a negative configurational entropy, inconsistent with the definition in Eq. (14).

The physically intuitive analogy for effective temperature, mean energy, $\bar{F}$, and configurational entropy to thermodynamic relations [Eq. (17)] suggests that one should analyze the corresponding *configurational heat capacity*,

$$C_c = T_{\text{eff}} \frac{\partial \overline{S_c}}{\partial T_{\text{eff}}} = -m \frac{\partial \overline{S_c}}{\partial m}. \quad (18)$$

Using distribution function (12) we find, as expected, that C_c is a measure of the fluctuations of the energy and configurational entropy of glassy states. We obtain for the configurational heat capacity,

$$C_c = \frac{\overline{(\delta F)^2}}{T_{\text{eff}}^2} = \overline{(\delta S_c)^2}, \quad (19)$$

where $\overline{(\delta F)^2} = \overline{F^2} - \bar{F}^2$ and $\overline{(\delta S_c)^2} = \overline{S_c^2} - \overline{S_c}^2$. Here the mean values $\bar{F}$ and $\overline{S_c}$ are determined by Eq. (17). The fluctuations of the configurational entropy and frozen state energy are then determined by $\overline{S_c^2} = \int D\hat{\rho} P[\hat{\rho}] \log^2 P[\hat{\rho}]$ and $\overline{F^2} = \int D\hat{\rho} P[\hat{\rho}] f[\hat{\rho}]^2$, respectively. Both quantities can be expressed within the replica formalism in terms of a second derivative of $F(m)$ with respect to m. For example, it follows that

$$\frac{\partial^2}{\partial m^2} m F(m) = -\frac{1}{T} (\overline{F^2} - \bar{F}^2). \quad (20)$$

It is then easy to show that Eq. (19) holds. With the introduction of the configurational heat capacity into the formalism we have a measure for the fluctuation of the number of available metastable states from its mean value. The analogy of these results to the usual fluctuation theory of thermodynamic variables[34] further suggests that C_c also determines fluctuations of the effective temperature with mean-square deviation,

$$\overline{(\delta T_{\text{eff}})^2} = T_{\text{eff}}^2 / C_c. \quad (21)$$

Since C_c is extensive, fluctuations of intensive variables, such as T_{eff}, or densities, such as $s_c = S_c / V$, vanish for infinite systems. However, they become relevant if one considers finite subsystems or small droplets. In the context of glasses this aspect was first discussed by Donth.[35]

Using standard techniques of many-body theory we can proceed by expressing the replica free energy $F(m)$ as a functional of the liquid correlation functions of the problem (see, e.g., Ref. 36)

$$H[\chi] = \frac{T}{2m} [\text{Tr}(\chi_0^{-1} \chi) + T \, \text{Tr} \ln \chi + \Phi[\chi]]. \quad (22)$$

Here the mean-field result of $F(m)$ is determined by the stationary point of the effective Hamiltonian: $\frac{\delta H}{\delta \chi} = 0$ with replicated density-density correlation function,

$$\chi_{ab}(x,x') = \langle \delta \rho_a(x) \delta \rho_b(x') \rangle. \quad (23)$$

The Luttinger-Ward functional $\Phi[\chi]$ is determined by the nature of the density-density interaction and determines the self-energy $\Sigma = -\frac{\delta \Phi}{\delta \chi}$; see also Refs. 4 and 37. For example, expanding the density functional, $\phi(\rho) = \phi(\rho_0 + \delta\rho)$, into a Taylor series in $\delta\rho$ yields to lowest order in $\delta\rho$,

$$\Phi = -\frac{v_3^2}{3} \int d^d x d^d x' \sum_{ab} \chi_{ab}^3(\mathbf{x}, \mathbf{x}'), \quad (24)$$

where $v_3 = \frac{1}{2} \frac{d^3 \phi(\rho_0)}{d \rho_0^3}$.[38] In what follows we will formulate the theory in terms of the collective variable $\chi_{ab}(\mathbf{x}, \mathbf{x}')$, instead of the original density fluctuations and write

$$\chi_{ab}(\mathbf{x}, \mathbf{x}') = \chi(\mathbf{x}, \mathbf{x}') \delta_{ab} + C_{ab}(\mathbf{x}, \mathbf{x}'), \quad (25)$$

where $C_{ab} = 0$ if $a = b$. $C_{ab}(\mathbf{x}, \mathbf{x}')$ depends on two spatial variables x and x'. We simplify the problem by assuming that its

Fourier transformation, $C_{ab}(\frac{\mathbf{x}+\mathbf{x}'}{2},\mathbf{q})$, with respect to the relative coordinates $x-x'$ can be written as

$$C_{ab}(\mathbf{r};\mathbf{q}) = q_{ab}(\mathbf{r})\rho_0 S(\mathbf{q}), \tag{26}$$

with liquid structure factor; $S(\mathbf{q})$ and $\mathbf{r}=(\mathbf{x}+\mathbf{x}')/2$ is the center of mass coordinate. The important collective variable of our theory is $q_{ab}(\mathbf{r})$, which plays the role of a spatially varying Debye-Waller factor. Within mean-field theory we expect below the temperature T_A that $q_{ab}=q^*(1-\delta_{ab})$ is replica symmetric with q^* of order unity, while q^* vanishes in the equilibrium liquid state for $T>T_A$. Physically the Debye-Waller factor q^* contains the same information as does the localization parameter α^{-1} discussed above. Finally, it is important to stress that a replica symmetric approach of q_{ab} in the present formalism is equivalent to one step replica symmetry breaking in the conventional replica language.[28]

In order to keep our calculation transparent we will not determine $H[q]$ from an explicit microscopic calculation for supercooled liquids. It was demonstrated by Franz and Parisi[39] that this is possible. However, in order to be able to make simple calculations beyond the mean-field theory explicitly including droplet fluctuations, we start from a simpler Landau theory in the same universality class,[20,40]

$$H = E_0 \sum_{a,b} \int \frac{d^3r}{a_0^3}\left(h[q_{ab}] - \frac{u}{3}\sum_c q_{ab}q_{bc}q_{ca}\right), \tag{27}$$

with

$$h[q_{ab}] = \frac{a_0^2}{2}(\nabla q_{ab})^2 + \frac{t}{2}q_{ab}^2 - \frac{u+w}{3}q_{ab}^3 + \frac{y}{4}q_{ab}^4 \tag{28}$$

and replica index $a,b=1,\ldots,m$. a_0 is a length scale of the order of the first peak in the radial distribution function of the liquid, and E_0 is a typical energy of the problem that determines the absolute value of $T\overline{s_c}$. In addition the problem is determined by the dimensionless variables t, u, w, and y, which are in principle all temperature dependent. We assume that the primary T dependence is that of the quadratic term, where $t=\frac{T-T_0}{E_0}$. Making this assumption, along with the polynomial form of the Lagrangian, requires constraints between the other Landau parameters to ensure thermodynamic consistency from the fluctuation formulas. In Appendix A we give estimates for the parameters of Eqs. (27) and (28) obtained from fits to experimental data for OTP, a well-studied fragile glass-forming material. Formally, Eqs. (27) and (28) can be motivated as the Taylor expansion of Eq. (22) together with the functional Φ of Eq. (24). In what follows we further simplify the notation and measure all energies in units of E_0 and all length scales in units of a_0.

The mean-field analysis of this model Hamiltonian is straightforward. Inserting a replica symmetric ansatz $q_{ab}=q^*(1-\delta_{ab})$ into H and minimizing with respect to q^* yield $q^*=0$ or

$$q^* = \frac{w+\sqrt{w^2-4ty}}{2y}. \tag{29}$$

Nontrivial solutions exit for $t<t_A=\frac{w^2}{4y}$ with $q^*(t_A)=\frac{w}{2y}$, which determines the mode-coupling temperature $T_A=t_AE_0+T_0$. Inserting q^* of Eq. (29) into $H[q]$ yields for the replica free energy

$$\frac{F(m)}{V(m-1)} = \frac{t}{2}q^{*2} - \frac{w+u(m-1)}{3}q^{*3} + \frac{y}{4}q^{*4}. \tag{30}$$

The mean configurational entropy density, as determined by $\overline{s_c}=\frac{1}{TV}\frac{\partial}{\partial m}F(m)|_{m\to 1}$, is given by

$$T\overline{s_c} = \left(\frac{t}{2}q^{*2} - \frac{w}{3}q^{*3} + \frac{y}{4}q^{*4}\right). \tag{31}$$

Inserting q^* of Eq. (29) yields the result that $\overline{s_c}$ vanishes at $t_K=\frac{2w^2}{9y}$ with $q^*(t_K)=\frac{2w}{3y}$. Close to t_K it follows that

$$\overline{s_c} \simeq \frac{t_K}{4y}\left(\frac{t-t_K}{T_K}\right) \propto \frac{T-T_K}{T_K} \tag{32}$$

as expected. At t_A one finds $T_As_c(T_A)=\frac{w^4}{192y^3}$.

We next determine the configurational heat capacity of the mean-field theory discussed above. From Eq. (30) we obtain

$$C_c = \frac{2Vm}{T_{\text{eff}}}\left(\frac{t}{2}q^{*2} - \frac{w-u(2-3m)}{3}q^{*3} + \frac{y}{4}q^{*4}\right). \tag{33}$$

If $T_{\text{eff}}=T$ (corresponding again to the equilibrium behavior between T_K and T_A) it follows that $C_c(T_K)=\frac{Vu}{T_K}\frac{2}{3}(\frac{2w}{3y})$ (Ref. 41) so that comparing it with the expression for the configurational entropy [Eq. (31)] at $t\simeq t_K$ we can write it as

$$\overline{S_c} \simeq \frac{w}{4u}C_c(t_K)\frac{t-t_K}{t_K}. \tag{34}$$

Notice that $w/4ut_K$ must equal $1/T_K$ for complete thermodynamic consistency. For temperatures close to but above T_K the energy fluctuations decrease as

$$C_c \simeq C_c(t_K)\left(1 - \frac{8u+w}{2}\frac{t-t_K}{t_K}\right). \tag{35}$$

As the temperature approaches T_A the configurational heat capacity decreases faster than linearly. It reaches a value $C_c(t_A)=\frac{V}{T_A}\frac{8u-w}{96}\frac{w^3}{y^3}$ signaling that the system becomes unstable close to t_A for $w>8u$. This is analogous to the higher order replica symmetry breaking suggested by Tarzia and Moore[42] on the basis of the same Landau action. $C_c(t\to t_A)$ approaches $C_c(t_A)$ from above with an infinite slope,

$$\frac{C_c(t\to t_A)}{C_c(t_A)} = 1 - \frac{24\left(\frac{t_A-t}{t_A}\right)^{1/2}}{8u-w}. \tag{36}$$

The full temperature dependences of the mean-field overlap q^* and configurational heat capacity are shown in Fig. 3. While q^* or $\overline{s_c}$ did not depend on the parameter u of the Hamiltonian [Eqs. (27) and (28)], the configurational heat capacity did. We may therefore consider u as a parameter that determines the strength of entropy fluctuations.

B. Effective potential approach

In order to investigate the transition state for the decay of a specific metastable frozen state, it is necessary to have a

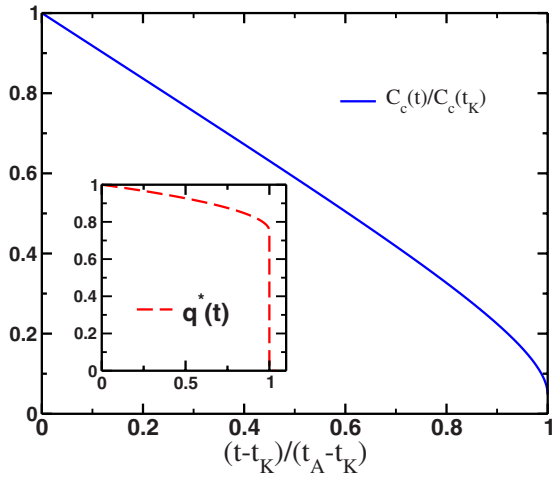

FIG. 3. (Color online) Mean-field value for the configurational heat capacity (main plot) and overlap (inset) for $y=1.82$, $w=2.72$, $u=0.385$ (see text) as a function of reduced temperature $(t-t_K)/(t_A-t_K)$. Exponentially many states emerge below t_A with the discontinuous jump of the overlap.

technique that agrees with the mean-field replica approach discussed in the previous section in case of a homogeneous solution $q=q^*$ but that allows one to study the behavior for arbitrary values of the overlap between two states, including inhomogeneous droplet solutions. This is possible within the effective potential approach introduced in Refs. 18, 39, and 43. We use this technique to formulate our replica instanton and barrier fluctuation theory.

We are interested in the regime above T_K (i.e., for $t>t_K$) and consider the partition function of a system with constrained overlap between the particle density configurations $\rho_1(\mathbf{r})$ and $\rho_2(\mathbf{r})$,

$$Z_{p_c,\rho_2} = \int D\rho_1 e^{-\beta\phi[\rho_1]} \times \prod_{\mathbf{x}} \delta(p_c(\mathbf{r}) - \rho_2(\mathbf{r})\rho_1(\mathbf{r})). \quad (37)$$

The configuration ρ_2 is assumed to be in equilibrium and unaffected by ρ_1. Averaging the free energy, $-T\log Z_{p_c,\rho_2}$, weighted with the equilibrium probability for ρ_2 yields the corresponding mean energy for the overlap p_c,

$$\Omega[p_c] = -T\langle \log Z_{p_c,\rho_2}\rangle_{\rho_2} = -T\frac{\int D\rho_2 e^{-\beta\phi[\rho_2]} \log Z_{p_c,\rho_2}}{Z}. \quad (38)$$

Here Z is the equilibrium partition function $Z=\int D\rho e^{-\beta\phi[\rho]}$. Using a replica approach $\Omega[p_c]$ can be written as[18]

$$\Omega[p_c] = -T\lim_{n\to 0}\lim_{m\to 0}\frac{1}{m}(Z^{(n,m)}-1), \quad (39)$$

with

$$Z^{(n,m)} = \int D^n\rho D^m\hat{\rho} e^{-\beta\Sigma_{\alpha=1}^n\phi[\rho_\alpha]-\beta\Sigma_{b=1}^m\phi[\hat{\rho}_b]} \times \prod_{r,b=1}^{m}\delta(p_c(r)-\rho_1(r)\hat{\rho}_b(r)). \quad (40)$$

$\Omega[p_c]$ can be determined by analyzing an $n+m$ times replicated problem with additional constraint for the overlap between certain replicas. In complete analogy to the previous paragraph one can introduce a field theory of the overlap but now with order parameter

$$Q = \begin{pmatrix} r & p \\ p^T & q \end{pmatrix}, \quad (41)$$

where r is an $n\times n$ matrix, q an $m\times m$ matrix, and the $n\times m$ matrix p must obey the additional constraint that $p_{1b}(r)=p_c(r)$ for $\forall_{b=1,\ldots,m}$. We have the same effective Hamiltonian [Eqs. (27) and (28)] only with q replaced by Q; i.e.,

$$\overline{Z^{(n,m)}} = \int DQ e^{-\beta H[Q]}\prod_{b=1}^{m}\delta(p_{1b}-p_c). \quad (42)$$

Following Franz and Parisi[18] we use $r_{\alpha\beta}=0$ and $p_{ab}=\delta_{\alpha,1}p_c$ and it follows that

$$H_{p_c}[q] = \int d^dr\left(2mh[p_c] + \sum_{ab}h[q_{ab}] - \frac{u}{3}\sum_{abc}q_{ab}q_{bc}q_{ca} - up_c^2\sum_{bc}q_{bc}\right). \quad (43)$$

The remaining q_{ab}-dependent problem is formally similar to the original one of Eqs. (27) and (28) but in an external field up_c^2.

Using these results we find that the effective potential can be written as

$$\Omega[p_c] = 2\int d^dr h[p_c] + \tilde{\Omega}[p_c], \quad (44)$$

with

$$\tilde{\Omega}[p_c] = -\frac{\partial}{\partial m}\int Dq e^{-\beta H_{p_c}[q]}\Big|_{m\to 0}. \quad (45)$$

We start with a homogeneous replica symmetric ansatz for $q_{ab}=q(\delta_{ab}-1)$ with equal off diagonal elements, q, and zero diagonal elements. It was demonstrated that this replica symmetric ansatz is again equivalent to one step replica symmetry breaking in the conventional replica language.[44] We take the limit $m\to 0$ and find

$$\frac{H_{p_c}(q)}{Vm} = -h(q) + 2h(p_c) + up_c^2q - \frac{2}{3}uq^3. \quad (46)$$

If we extremize this with respect to q, i.e., perform the integration with respect to q at the level of a homogeneous saddle-point approximation, it follows that

$$tq - (w-u)q^2 + yq^3 = up_c^2. \tag{47}$$

Depending on the value for the overlap p_c, q is in general different from the value q^* obtained within the replica approach of the previous section. If we however insert q back into $H_{p_c}(q)$ and determine the effective potential $\Omega[p_c] = H_{p_c}(q(p_c))$ we find that it has minima $\frac{\partial\Omega[p_c]}{\partial p_c}=0$ for $p_c=0$ and for $p_c=q(p_c)=q^*$, with q^* of Eq. (29), in complete agreement with the approach of the previous section. The value of the effective potential for the metastable minimum $p_c=q^*$ is identical to the mean configurational entropy discussed above,

$$\Omega[q^*] = \overline{S_c}. \tag{48}$$

In order to analyze the local stability of the solution at the minimum of $\Omega(p_c)$ we determine the replicon eigenvalue of the problem. Following Ref. 45 gives

$$\lambda_r = t - 2wq + 3yq^2 \tag{49}$$

for the lowest eigenvalue. Inserting q from Eq. (47) yields close to t_K a positive eigenvalue: $\lambda_r \simeq t_K - 5(t-t_K)$, while the replicon eigenvalue vanishes at t_A as $\lambda_r \simeq 2t_A(\frac{t_A-t}{t_A})^{1/2}$. This behavior is completely consistent with the results obtained in Ref. 46 for the random Potts model. The homogeneous solution is marginal at T_A and stable below T_A. Except for temperatures close to T_A, the mean-field approach is locally stable with respect to small fluctuations. The effective potential approach is not restricted to overlaps p_c that minimize $\Omega[p_c]$. In general $q(p_c)$ is given by the solution of Eq. (47). Inserting this solution into $H_{p_c}(q)$ gives $\Omega(p_c)$. The result is shown as broken line in Fig. 6. It turns out that for intermediate values of p_c, between $p_c=0$ and $p_c=q^*$ an additional replica symmetry breaking of q_{ab} occurs.[43] For the present model this effect was also studied in Ref. 20. This is related to the well-known effect that an external field can cause replica symmetry breaking above T_K,[47] yielding one step replica symmetry breaking for q_{ab}. The result for $\Omega(p_c)$ shown in Fig. 4 has been obtained, including this additional replica symmetry breaking. Physically this additional replica symmetry breaking as p_c "goes over the hill" was discussed in Ref. 20. We also note that the generic behavior for $\Omega(p_c)$ as shown in Fig. 4 is very similar to $T\overline{s_c}(q^*)$ of Eq. (31) if we simply plot this function for arbitrary q^*. As required both expressions exactly agree at saddle points and minima.

In summary, we showed that on the level of spatially homogeneous mean-field solutions, the effective potential approach of Refs. 18, 39, and 43 yields results in complete agreement with the physically transparent approach of Ref. 28. Since it allows for arbitrary overlap between two states, we use it as starting point for the determination of activated events within an instanton calculation.

C. Instanton theory for activated events

At the mean-field level a glass at $T<T_A$ is frozen in metastable states and characterized by the overlap q^* of Eq. (29) between configurations at distant times. For temperatures $T>T_K$ above the Kauzmann temperature, the free energy of such a frozen state is higher by the configurational entropy $T\bar{S}_c$ compared to the liquid state that is characterized by $q^*=0$. Thus, for $T_K<T<T_A$ the mean-field glass is locally stable (the replicon eigenvalue λ_r is positive) but globally unstable with respect to the ergodic liquid. The effective potential $\Omega(p_c)$ shown in Fig. 3 suggests that the decay modes for the frozen state are droplet excitations, similar to the nucleation of an unstable phase close to a first-order transition. This situation was analyzed in Refs. 19 and 20. Using this approach, an analysis of the effective droplet size for a Kac-type model was performed in Ref. 48. In agreement with the RFOT theory,[8] the driving force for nucleation is the configurational entropy, leading to the notion of entropic droplets. We stress that the variation in the "origin of the instanton" is included in our formalism. In the instanton calculations one always considers a noninteracting gas of infinitely many (but dilute) instantons that are distributed in space with arbitrary origin. The statistical weight of one instanton that is forced to be at a fixed location would be vanishingly small.

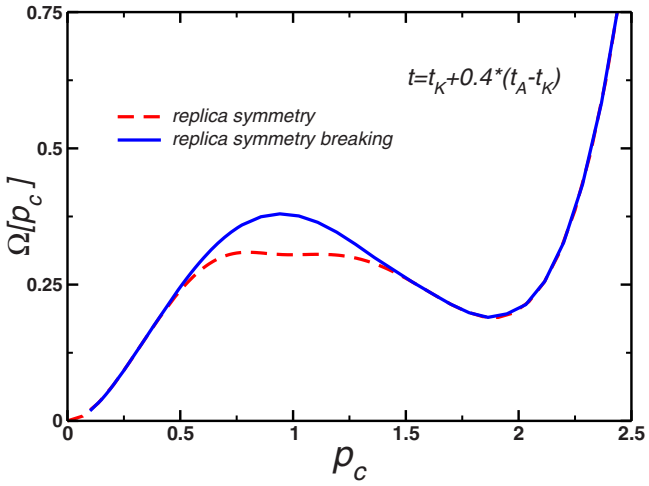

FIG. 4. (Color online) Effective potential $\Omega[p_c]$ as a function of the overlap at the fixed temperature $T_K<T<T_A$. At the Kauzmann temperature an entropy crisis takes place with vanishing entropic advantage of the liquid compared to the frozen solid.

Instanton solutions for entropic droplets are determined from

$$\frac{\delta\Omega[p_c]}{\delta p_c(\mathbf{r})} = 0, \tag{50}$$

where we allow for spatial variations in the overlap $p_c(\mathbf{r})$.[49] Recently, Franz[50] gave a transparent dynamical interpretation for the solutions of Eq. (50). Assuming that the effective potential is characterized by spatially anisotropic but replica symmetric solutions $q_{ab}(\mathbf{r})=q(\mathbf{r})(\delta_{ab}-1)$, we perform the integral over the q_{ab} in Eq. (45) at the saddle-point level. We find a solution $q(\mathbf{r})=p_c(\mathbf{r})$ with

$$\nabla^2 p_c(\mathbf{r}) = \frac{dV[p_c(\mathbf{r})]}{dp_c(\mathbf{r})}, \tag{51}$$

where

$$V(p_c) = \frac{t}{2}p_c^2 - \frac{w}{3}p_c^3 + \frac{y}{4}p_c^4. \tag{52}$$

Equation (51) admits an exact solution in the thin-wall limit $R \gg \xi$,

$$p_c(r/\xi) = q^* + \sqrt{\frac{2}{y\xi^2}}\left[\mathrm{th}\left(\frac{r}{\xi} - z_0\right) - \mathrm{th}\left(\frac{r}{\xi} + z_0\right)\right], \tag{53}$$

where the integration constant z_0 is a function of t, w, and y. R is the droplet radius and ξ is the interface width given by

$$\xi = \frac{4a_0}{\sqrt{3y(2q^* - q_K^*)^2 - 6t_K + 4t}}. \tag{54}$$

The final expression for the function $z_0(t)$ is more involved and is given in Appendix C.

Inserting solution (53) into the expression for the effective potential [Eq. (44)] we calculate the value of the mean barrier. The latter is determined by optimizing the energy gain due to creation of a droplet and energy loss due to the surface formation. As a result for the most probable barrier we find (reintroducing the energy scale E_0 and length scale a_0)

$$\overline{F^\ddagger} = E_0 \frac{32\pi a_0}{9y\xi^3} R^2. \tag{55}$$

The droplet radius,

$$R = \frac{64a_0^4}{3y^2 q^{*3}(q_K^* - q^*(t))\xi^3}, \tag{56}$$

is determined from the balance between the interface tension and the entropic driving force for nucleation. The barrier energy $\overline{F^\ddagger}$ of Eq. (55) determines the relaxation time $\bar{\tau}$ of Eq. (2). Furthermore, $q_K^* \equiv q^*(t=t_K)$ is the order parameter at the Kauzmann temperature. When temperature approaches the T_K the radius of the droplet as well as the most probable barrier diverge. One finds $\lim_{t\to t_K} \overline{F^\ddagger} \propto (t-t_K)^{-2}$ and $\lim_{t\to t_K} R \propto (t-t_K)^{-1}$. Since the droplet interface ξ remains finite as $t \to t_K$, the thin-wall approximation is well justified close to the Kauzmann temperature. On the other hand, R and ξ become comparable for temperatures close to T_A and the thin-wall approximation breaks down. We see that replica Landau functional calculation predicts a rather diffuse droplet near the laboratory T_g. Combining $R \propto (t-t_K)^{-1}$ and $\overline{s_c} \propto (t-t_K)$, we obtain $\nu=1$ for the exponent that relates the droplet size R and the configurational entropy density: $R \propto s_c^{-\nu}$.

In Ref. 51 it was demonstrated that for a similar model the interface free energy is exponentially small for a large system, and in any finite dimension the one step replica symmetry breaking state does not exist. As was already pointed out in Ref. 51, our approach is very different in scope and in its conclusions. While Ref. 51 is concerned with the absence of replica symmetry breaking in the ultimate equilibrium state, our conclusions are relevant for the nonequilibrium situation. Since we obtain a finite barrier height of the frozen mean-field solution, our result offers a mechanism for equilibration on time scales $t \gg \bar{\tau}$ demonstrating that our approach and the conclusions of Ref. 51 are consistent.

D. Barrier fluctuations

To analyze the barrier fluctuations we start from the barrier for a given density configuration ρ,

$$F^\ddagger_{p_c,\rho} = F_{p_c,\rho} - F_{q^*,\rho}, \tag{57}$$

where $F_{p_c,\rho} = -T \log Z_{p_c,\rho}$ is determined by the constrained partition function of Eq. (37) and $F_{q^*,\rho}$ is the corresponding energy with homogeneous overlap; i.e., $F_{q^*,\rho} = -T \log Z_{p_c(r\to\infty)\to q^*,\rho}$. When we analyze variations in activation barriers we need to keep in mind that both ground-state and transition state contributions to $F^\ddagger_{p_c,\rho}$ are statistically fluctuating and are correlated in general. Fluctuations in the first term of Eq. (57) correspond to variations in the free energy of the localized instanton. On the other hand, fluctuations in the second term correspond to variations in the homogeneous background. In principle cancellations between both occur, which are properly included in the analysis of $F^\ddagger_{p_c,\rho}$ defined above.[52]

Barrier fluctuations are then characterized by the second moment,

$$\overline{\delta F^{\ddagger 2}} = \overline{F^{\ddagger 2}_{p_c,\rho}} - \overline{F^\ddagger_{p_c,\rho}}^2, \tag{58}$$

where the average is, just as for the analysis of the most probable barrier, with respect to the density configuration ρ. The second term in Eq. (58) is the square of the mean activation barrier $\overline{F^\ddagger}$ and was determined in the previous section. Thus, we can concentrate on the first term. Using Eq. (57) it follows that the first term in Eq. (58) consists of three terms,

$$\overline{F^{\ddagger 2}_{p_c,\rho}} = \overline{F^2_{p_c,\rho}} + \overline{F^2_{q^*,\rho}} - 2\overline{F_{p_c,\rho}F_{q^*,\rho}}. \tag{59}$$

In what follows we consider these three contributions separately. The first two terms correspond to independent fluctuations of the droplet and the homogeneous background, while the last term measures their mutual correlations. In other words, our approach explicitly takes the fluctuations of the initial configuration [second term in Eq. (59)] and the cross correlations between the localized instanton and the initial configuration [third term in Eq. (59)] into account. We find that this last term in Eq. (59) is proportional to the surface area of the instanton. Correlations between droplet and homogeneous background terms result from their mutual interface.

The detailed analysis of the three contributions to $\overline{F^{\ddagger 2}_{p_c,\rho}}$ of Eq. (59) is summarized in Appendix B. In what follows we summarize the results of this derivation. For the first two terms in Eq. (59) it follows that

$$\overline{F^2_{q^*,\rho}} = \overline{F_{q^*,\rho}}^2 - 2T\int d^3\mathbf{r} h[q^*],$$

$$\overline{F^2_{p_c,\rho}} = \overline{F_{p_c,\rho}}^2 - 2T\int d^3\mathbf{r} h[p_c(\mathbf{r})]. \tag{60}$$

The first expression gives fluctuations of the configurational entropy for the homogeneous problem, while the second one describes the energy fluctuations of the configurations with spatially heterogeneous overlap.

The result for the homogeneous problem, $\overline{F^2_{q^*,\rho}}$ can alternatively be obtained from our analysis of the configurational heat capacity given in Eq. (19). Using the replica formulation of Eq. (20) together with the explicit result of Eq. (30) yields

$$\overline{F^2} - \bar{F}^2 = -2VT\left(\frac{t}{2}q^{*2} - \frac{w+u}{3}q^{*3} + \frac{y}{4}q^{*4}\right), \quad (61)$$

where V is the volume. If we now recall the definition of $h[q]$ [Eq. (28)], one readily observes that the first equation in Eq. (60) coincides with Eq. (61).

The derivation of the third contribution $\overline{F_{p_c,\rho}F_{q^*,\rho}}$ to $\overline{F^{\ddagger 2}_{p_c,\rho}}$ in Eq. (59), which describes the energy correlations between the instanton and environment, is also performed in Appendix B. The result is

$$\overline{F_{p_c,\rho}F_{q^*,\rho}} = \overline{F_{p_c,\rho}} \times \overline{F_{q^*,\rho}} - T\int d^3\mathbf{r}\{2h[p_c(\mathbf{r})] + up_c^3(\mathbf{r}) - uq^* p_c(\mathbf{r})\}. \quad (62)$$

Combining Eq. (60) with Eq. (62), we finally obtain for the second moment of the barrier fluctuations,

$$\frac{\overline{\delta F^{\ddagger 2}}}{2T} = \int d^3r(h[p_c] - h[q^*] + up_c^3(\mathbf{r}) - uq^* p_c^2(\mathbf{r})). \quad (63)$$

This result for the second moment of the barrier fluctuations depends on the value of the homogeneous overlap q^* of Eq. (29) as well as the instanton solution $p_c(\mathbf{x})$. The thin-wall limit result for $p_c(\mathbf{x})$ is given in Eq. (53). Inserting these expressions into Eq. (63) yields

$$\overline{\delta F^{\ddagger 2}} = A(R^3 + \rho R^2), \quad (64)$$

where R is the radius of the droplet. In the thin-wall approximation, the explicit expression for the coefficient A is

$$\frac{A}{k_B T E_0} = \frac{2\pi y}{3a_0^3}\left[-\left(1+\frac{u}{w}\right)(q^{*3} - q_1^3) + q^{*4} - q_1^4 + \frac{2u}{y}(q_1^3 + q^{*3} - 2q_1^2 q^*)\right], \quad (65)$$

where the value of q_1 is computed using an effective potential $V(q_1) = V(q^*)$; i.e., it is the turning point of the instanton (see Fig. 3). Deriving Eq. (65) we also made the following choice for the parameters $q^*(t_K) = 2w/3y = 1$ (see Appendix A for more details). This choice is of particular convenience as it allows one to express the resulting expressions in terms of the ratio t/t_K and u. The length scale $\rho(t)$ can be compacted as follows:

$$\rho(t) = \frac{4\pi t_K \xi(t)}{a_0^3}\left(\frac{k_B T E_0}{A}\right) \times \left[\frac{2uq^*}{t_K}c_2(t) - \left(1+\frac{4u}{3t_K}\right)c_3(t) + c_4(t)\right], \quad (66)$$

where $c_n(t)$ are functions of the ratio t/t_K only and are defined via

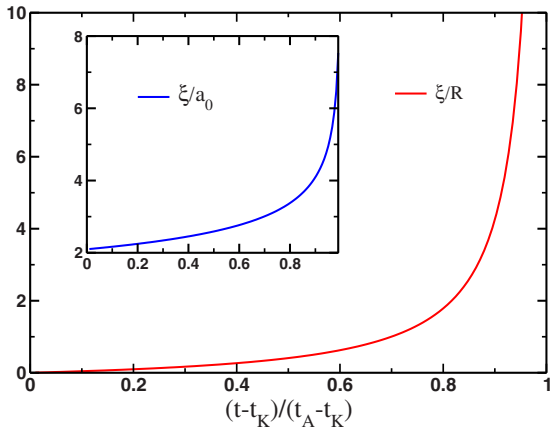

FIG. 5. (Color online) We show the temperature dependence of the ratio ξ/R (R is the size of the droplet) together with the temperature dependence of interface width $\xi(t)$ (inset).

$$c_n(t) = \int_0^\infty [q^{*n} - p_c^n(z)]dz. \quad (67)$$

We have computed these integrals numerically for $n=2$, 3, and 4. Temperature dependence of the surface length scale $\rho(t)$ is shown in Fig. 5.

Before we proceed with the analysis of our results, it is instructive to write down the expressions for the coefficient A and $\rho(t)$ for temperatures close to t_K. When $t \simeq t_K$, one readily finds $q_1 \simeq t_K(t-t_K)/y$ so that expanding expression in the square brackets Eq. (65) up to the linear order in $t-t_K$ we have $A(t) \simeq (k_B T E_0/a_0^3)[A_0 + A_1(t-t_K)] + \mathcal{O}((t-t_K)^2)$ with

$$A_0 = \frac{8\pi}{9}u, \quad A_1 = 4\pi\left(\frac{2u}{t_K} + 1\right), \quad (68)$$

where once again we employed $q^*(t_K) = 1$ (see Appendix A). Thus we find that close to t_K the bulk contribution to the barrier fluctuations is governed solely by the value of the phenomenological parameter u. The expression for $\rho(t \simeq t_K) = \rho_K + \rho_{1K}(t-t_K)$ can be derived straightforwardly using our results above together with the expansion for the functions $c_n(t)$ and $\xi(t) \simeq 2/\sqrt{t_K} + 5(t-t_K)/t_K^{3/2}$. Here we provide the expression for the value of $\rho(t=t_K)$,

$$\rho(t_K) = \frac{9t_K^{1/2}}{u}\left[c_{4K} - c_{3K} + \frac{2u}{t_K}\left(c_{2K} - \frac{2}{3}c_{3K}\right)\right], \quad (69)$$

where we have used the notations $c_{nK} \equiv c_n(t_K)$. We have found that the coefficients c_{nK} have the following values: $c_{2K} \simeq 1.25$, $c_{3K} \simeq 1.18$, and $c_{4K} \simeq 1.11$.

Thus, in addition to the bulk term, which behaves in a similar way as the formulation in Ref. 12 [see Eq. (9)], the replica theory yields a surface term, resulting from fluctuations in the interface. In the inset of Fig. 6 we show the T dependence of the length scale $\rho(t)$, demonstrating that the surface term becomes gradually more important as the temperature increases. The value of $\rho(t_K)$ remains nonsingular so that the volume term is dominant. This is consistent with the view that the droplet interface close to T_K is smaller then the droplet radius, while both are comparable as T approaches

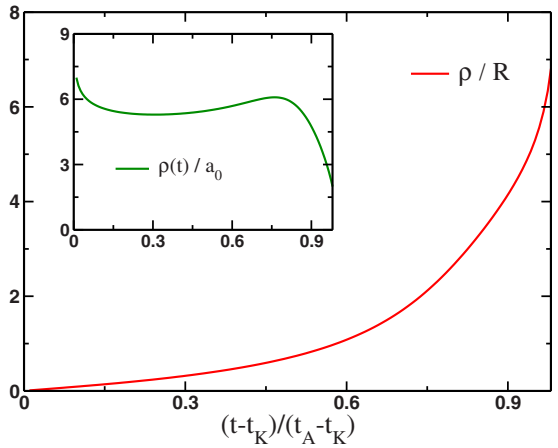

FIG. 6. (Color online) Temperature dependence of the length scale $\rho(t)$ describing the contribution to the barrier fluctuations due to surface energy fluctuations of the structural droplets. We also show the temperature dependence of the ratio ρ/R (R is the size of the droplet).

T_A, similar to the behavior close to a spinodal.[53] The resulting temperature dependence of $\rho(t)$ is shown on Fig. 6, $\overline{\delta F^{\ddagger 2}}$ is shown in Fig. 7, and the exponent of the stretched exponential relaxation β_G is shown in Fig. 8.

The plots are constructed by setting the parameters of the theory to reproduce experimentally relevant values of T_K, T_g, and T_A, as well as configurational entropy above the glass transition using o-terphenyl as the example of the glass transition (see Appendix A for details). There is one free parameter left to be fixed, either y or $w=3y/2$. We have determined the value of y in the comparison with the experimental value of the most probable barrier at $T=T_g$ given by $\overline{F^{\ddagger}}=T_g s_c(T_g)$ with the theoretically derived expression [Eq. (55)]. This procedure yields $y=1.82$, $w=2.73$, and $u=0.385$. As we can see from Fig. 8, $\beta_G(T_g)\simeq 0.12$, a value significantly reduced compared to the exponential behavior where $\beta=1$. This value for β_G is lower than the experimentally found values of $\beta_{\exp}(T=T_g)\simeq 0.5$. This discrepancy may signal that the

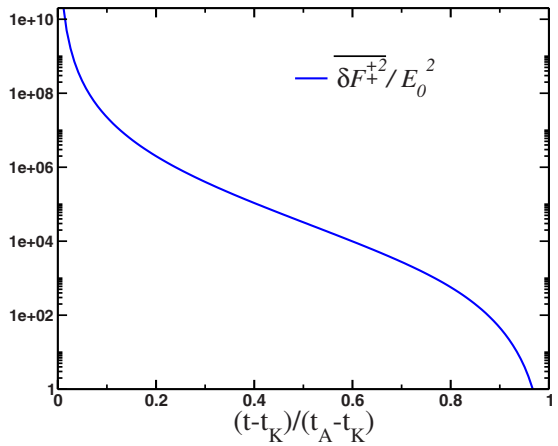

FIG. 7. (Color online) Temperature dependence of the energy barrier fluctuations.

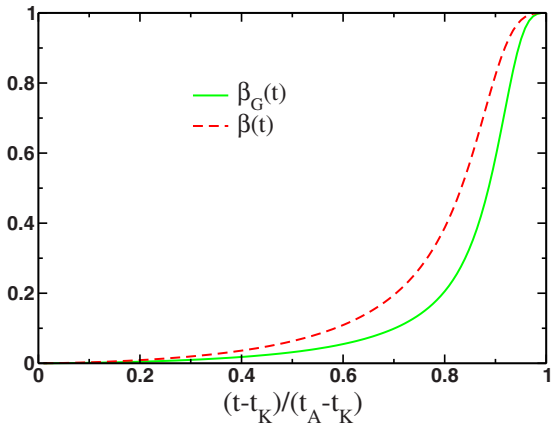

FIG. 8. (Color online) Temperature dependence of the exponent β_G governed by the fluctuations of the isolated droplets together with exponent β corrected by the effects of the droplet-droplet interactions.

present approach overestimates the strength of the energy barrier fluctuations, an effect that may be related with non-Gaussian fluctuations of the activation barriers. It is however clear that these may be described as instanton interaction effects as discussed by Xia and Wolynes.[11] Our analysis yields a Gaussian distribution of barriers,

$$P_G(F^{\ddagger}) = \frac{1}{\sqrt{2\pi\overline{\delta F^{\ddagger 2}}}}\exp\left(-\frac{(F^{\ddagger}-\overline{F^{\ddagger}})^2}{2\overline{\delta F^{\ddagger 2}}}\right), \tag{70}$$

which yields the following estimate for the exponent of the stretched exponential relaxation:

$$\beta_G = (1+\overline{\delta F^{\ddagger 2}}/(k_B T)^2)^{-1/2}. \tag{71}$$

Our results for the temperature dependence of β_G are shown in Fig. 8. The calculation that led to this result was based on the assumption of single instanton events; i.e., entropic droplets were assumed to be diluted. Obviously this is not addressing the fact that distinct droplets interact. The mosaic picture underlying the RFOT theory is clearly based on the view that such droplet-droplet interactions occur and are in fact crucial. The impact of droplet-droplet interactions for the distribution of barriers was analyzed in Ref. 11. Here it was pointed out that as soon as the droplet size becomes larger than the size R of a mean droplet [Eq. (55) in our theory], boundary effects will limit the size of a droplet, leading to a cutoff of the distribution function. This leads to the modified distribution function

$$P(F^{\ddagger}) = \begin{cases} \frac{1}{2}P_G(F^{\ddagger}) & F^{\ddagger} \le \overline{F^{\ddagger}} \\ \frac{1}{2}\delta(F^{\ddagger}-\overline{F^{\ddagger}}) & F^{\ddagger} > \overline{F^{\ddagger}} \end{cases}, \tag{72}$$

which leads to a reduction in the mean-square deviation of the barriers by a factor of 1/4, compared to the Gaussian distribution. This corrects the exponent of the stretched exponential relaxation to

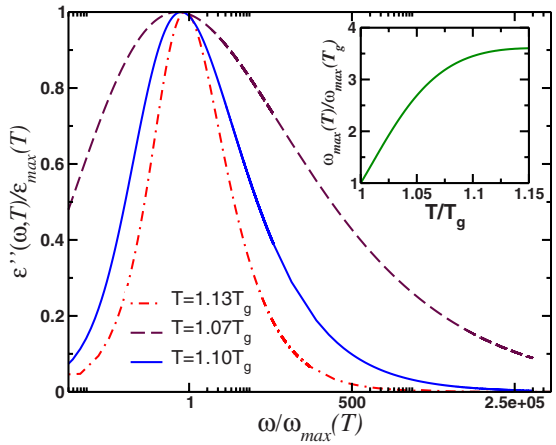

FIG. 9. (Color online) Frequency dependence of the imaginary part of the dielectric susceptibility above the glass transition. The broadening of the peak at the glass transition signals the appearance of wide spectrum of excitations.

$$\beta = \left(1 + \frac{1}{4}\overline{\delta F^{\ddagger 2}}/(k_B T)^2\right)^{-1/2}, \tag{73}$$

where $\overline{\delta F^{\ddagger 2}}$ is still the result [Eq. (63)] of the dilute droplet calculation. In Fig. 8 we compare β_G and β. Obviously, the reduction in the barrier fluctuation width due to droplet-droplet coupling leads to an increase in the exponent β. We mention however that the resulting value of β at the glass transition is $\beta(T_g) \simeq 0.23$. This suggests that the present Landau functional indeed overestimates the fluctuation effects. This probably implies that the diffuseness of the droplet from the Landau functional is also overestimated. The fluctuations do vanish at T_A, consistent with the emergence of simple exponential dynamics at a significantly high temperature. We did not attempt to vary the parameters of our model to reach perfect agreement with experiments for OTP as the simplified Landau functional is clearly an oversimplification of the physics of real glasses. It does however demonstrate the generic and qualitative trends for barrier fluctuations in the RFOT theory.

Finally, in Fig. 9 we show the dielectric function $\varepsilon''(\omega, T)$ as function of frequency for different temperatures. The peak in $\varepsilon''(\omega, T)$ dramatically broadens as temperature approaches the glass transition temperature, T_g, as predicted from the static barrier distributions.

For this figure we used the second moment $\overline{\delta F^{\ddagger 2}}$ of the barrier distribution function and then assumed that $p(F^{\ddagger})$ is Gaussian. In case of a Gaussian distribution, all moments can be expressed in terms of the second moment,

$$\overline{\delta F^{\ddagger k}} = \mu_k^G (\overline{\delta F^{\ddagger 2}})^{k/2}, \tag{74}$$

where $\mu_k^G = 0$ for k odd and $\mu_k^G = 2^k \Gamma(\frac{k+1}{2})/\sqrt{\pi}$ for k even. In particular it holds for higher order moments $\mu_3^G = 0$, $\mu_4^G = 3$, $\mu_5^G = 0$, and $\mu_6 = 15$, etc.

We can explicitly analyze higher moments of this distribution and thereby demonstrate explicitly that $p(F^{\ddagger})$ is Gaussian. To be precise, we have only shown this for the first six moments but strongly suspect this to be true in general. The calculations of higher moments are quite cumbersome but they formally are a straightforward generalization of the method we used to determine the second moment $\overline{\delta F^{\ddagger 2}}$. In case of the kth moment the block structure of the matrix Q of Eq. (B4) consists of $(k+1)\times(k+1)$ blocks where the total dimension of Q is $(n+\Sigma_{i=1}^k m_k)\times(n+\Sigma_{i=1}^k m_k)$. The rather tedious matrix algebra is then most easily analyzed using computer algebra software, such as MATHEMATICA. Thus, we only list the results here. We analyzed all moments,

$$\overline{\delta F^{\ddagger k}} = \int (F^{\ddagger} - \overline{F^{\ddagger}})^k p(F^{\ddagger}) dF^{\ddagger}, \tag{75}$$

up to $k=6$. We find

$$\overline{\delta F^{\ddagger 3}} = 0. \tag{76}$$

In case of the fourth moment we analyze

$$\overline{\delta F^{\ddagger 4}} = \overline{(F^{\ddagger}[\rho] - \overline{F^{\ddagger}})^4} = \overline{F^{\ddagger 4}[\rho_2]} - 4\overline{F^{\ddagger 3}[\rho_2]F^{\ddagger}} + 3\overline{F^{\ddagger}} + 6\overline{F^{\ddagger}F^{\ddagger 2}}. \tag{77}$$

It follows

$$\overline{\delta F^{\ddagger 4}} = 3[2\mathcal{V}[p_c; q_0] - \mathcal{H}_{\rm inh}[p_c] - \mathcal{H}_{\rm hom}(q^*)]^2, \tag{78}$$

where $\mathcal{H}_{\rm hom}$ and $\mathcal{H}_{\rm inh}$ are defined below Eq. (B8). Evaluating this expression yields

$$\overline{\delta F^{\ddagger 4}} = 3(\overline{\delta F^{\ddagger 2}})^2. \tag{79}$$

We further find that the fifth moment vanishes as well,

$$\overline{\delta F^{\ddagger 5}} = 0, \tag{80}$$

and that the sixth moment is given as

$$\overline{\delta F^{\ddagger 6}} = 15(\overline{\delta F^{\ddagger 2}})^3. \tag{81}$$

Thus, up to the sixth moment the barrier distribution of droplets is Gaussian. Thus, dilute entropic droplets should indeed have a Gaussian distribution of barriers, strongly suggesting that the observed non-Gaussian behavior of the effective barrier distribution results from droplet-droplet interactions.

III. SUMMARY

In summary, we have shown how the energy barrier fluctuations $\overline{\delta F^{\ddagger 2}}$ as well as higher moments of the static free-energy barrier distribution function $p(F^{\ddagger})$ can be computed using the replica Landau theory of Ref. 18 and use the replica instanton theory of Refs. 19 and 20. We have generalized the replica formalism to determine barrier fluctuations in addition to the determination of the most probable barrier $\overline{F^{\ddagger}}$. Barrier fluctuations $\overline{\delta F^{\ddagger 2}}$ consist of a dominating bulk contribution at temperatures close to the Kauzmann temperature along with a contribution stemming from fluctuations in the interface. The latter dominates the barrier fluctuations well above the Kauzmann temperature. Fluctuations of the surface energy enter prominently in the recent work of Biroli *et al.*[54] for directly computing point-to-set correlations in liquids. It is very nice to see that the effect they found naturally emerges from the replica instanton calculation framework. It is interesting to speculate that these surface energy fluctua-

tions could account for the observed system specific deviations from the Xia-Wolynes prediction of a direct relation between the stretching exponent and ΔC_v. Chemical trends in these deviations may provide clues on this. $\overline{\delta F^{\ddagger 2}}$ increases as the typical droplet size increases, i.e., as the temperature is lowered toward T_K. Clearly, our theory only applies until the system falls out of equilibrium at the laboratory glass temperature T_g with $T_g > T_K$. In the framework of the present instanton approach, the energy barrier distribution function turns out to be Gaussian. The skewness of the observed relaxation time distribution is, in our view, an effect due to the interaction of spatially overlapping instantons. It can be captured, at least in spirit, by an extended mode-coupling approach, incorporating instantons.

ACKNOWLEDGMENTS

This research was supported by the Ames Laboratory, operated for the U.S. Department of Energy by Iowa State University under Contract No. DE-AC02-07CH11358 (M.D. and J.S.), the Institute for Complex Adaptive Matter (M.D.), and the National Science Foundation [Grants No. CHE-0317017 (P.G.W.) and No. DMR 0605935 (M.D.)]. The authors also thank the Aspen Center for Physics, where part of this work was performed.

APPENDIX A: ESTIMATE OF THE MODEL PARAMETERS FOR O-TERPHENYL

The Landau functional is quite convenient for formal use, but there is a variety of ways that it may be mapped onto real fluids. In this appendix we show how the model parameters of the Landau replica potential [Eqs. (27) and (28)] can be found by fitting the results of the mean-field theory to experimental data. We use the concrete example o-terphenyl (OTP), a well-known glass-forming material. On one hand, values for the effective dynamical freezing temperature and the Kauzmann temperature of OTP are $T_A = 285$ K (Ref. 55) and $T_K = 202.7$ K.[56,57] On the other hand, a typical value for the glass temperature is[58] $T_g \simeq 243, \ldots, 246$ K. Here, the glass transition temperature is the temperature at which the viscosity reaches a value of 10^{13} g/(cm s), which is also where the mean relaxation time reaches values of 10^2 s. The melting temperature of OTP is $T_m = 329$ K with an entropy jump at melting of $\Delta S_m = 52.28 \frac{\mathrm{J}}{\mathrm{mol\ K}}$.

The configurational entropies at T_g and T_A are $S_c(T_g) = 21.5 \frac{\mathrm{J}}{\mathrm{mol\ K}} = 2.59R$ and $S_c(T_A) = 39 \frac{\mathrm{J}}{\mathrm{mol\ K}} = 4.69R$, respectively,[57,59] where R is the molar gas constant. To obtain the entropy per spherical object or bead one has to divide these results by $n_B = 3.7$, the number of beads as defined by the procedure in Ref. 14. This yields $s_c(T_g) \equiv \frac{S_c(T_g)}{n_B} = 0.7R$ as well as $s_c(T_A) = 1.26R$.

The heat capacity change at the glass transition is[60]

$$\Delta c_p(T_g) = 111.27 \frac{\mathrm{J}}{\mathrm{mol\ K}} = 0.48 \frac{\mathrm{J}}{\mathrm{g\ K}}, \tag{A1}$$

where we used 1 g $= 4.31 \times 10^{-3}$ mol. The specific and molar volumes of the system are[58]

$$v(T_A) = 0.918 \frac{\mathrm{cm}^3}{\mathrm{g}} = 213.2 \frac{\mathrm{cm}^3}{\mathrm{mol}},$$

$$v(T_g) = 0.893 \frac{\mathrm{cm}^3}{\mathrm{g}} = 207.3 \frac{\mathrm{cm}^3}{\mathrm{mol}}. \tag{A2}$$

The typical volume per particle $V/N = \frac{4\pi}{3} l_0^3$ is then characterized by the length l_0. It follows that $V/N = 344.23 \ddot{A}$ (Ref. 41) such that $l_0 = 4.35 \ddot{A}$. In comparison, the van der Waals radius of OTP was given as[61] $r_{\mathrm{vdW}} = 3.7 \ddot{A}$.

If we introduce the energy and length scales into the problem, the mean-field theory results obtained from Hamiltonian Eqs. (27) and (28) are

$$q_0(T_K) = \frac{2w}{3y},$$

$$T_A = T_0 \left(1 + \frac{E_0}{T_0} \frac{w^2}{4y} \right),$$

$$T_K = T_0 \left(1 + \frac{E_0}{T_0} \frac{2w^2}{9y} \right),$$

$$T_A s_c(T_A) = \frac{4\pi}{3} l_0^3 \frac{E_0}{a_0^d} \frac{w^4}{192 y^3},$$

$$s_c(T \simeq T_K) \simeq \frac{4\pi}{3} l_0^3 \frac{E_0 w}{6 T_K a_0^d} \left(\frac{2w}{3y} \right)^3 \frac{t - t_K}{t_K},$$

$$T_K c_c(T_K) = \frac{4\pi}{3} l_0^3 \frac{E_0}{a_0^d} \frac{2u}{3} \left(\frac{2w}{3y} \right)^3. \tag{A3}$$

The order parameter at T_K should be large in order unity. We chose $q_0(T_K) = 1$ which gives $w = \frac{3}{2} y$. Using the relation $T_A - T_K = \frac{w^2}{36y} E_0$ this yields

$$E_0 w = 1975.2 \ \mathrm{K} = 9.74 T_K. \tag{A4}$$

If we further make the reasonable choice of $a_0 = 0.87 r_{\mathrm{vdW}}$ for the length scale a_0, $s_c(T_A)$ of Eq. (A3) gives precisely the experimental value listed above. We can also determine the change in heat capacity $\Delta c_p(T_g)$ from the same parameters. Equation (A4) yields the result that

$$\frac{t - t_K}{t_K} \simeq 0.31 \frac{T - T_K}{T_K} \tag{A5}$$

so that we obtain for the temperature dependence of the configurational entropy

$$s_c(T) \simeq \Delta c_p(T_g) \frac{T - T_K}{T_g}, \tag{A6}$$

where the mean-field result for the slope is $\Delta c_p(T_g) = 4.36R$. This compares reasonably well with the experimental value $\Delta c_p(T_g) = \frac{\Delta C_p(T_g)}{n_B} = 3.62R$. Note, however, that Δc_p as given by Eq. (A6) is different from the configurational heat capacity c_c [Eq. (33)]. It holds that $s_c \simeq \frac{w}{4u} c_c(t_K) \frac{t - t_K}{t_K}$; i.e., $\frac{w}{4u} c_c(t_K) 0.253$

TABLE I. Parameters for the Landau functional.

$\frac{a_0}{r_{dv}w}$	$\frac{t_A}{t_K}$	$\frac{t_g}{t_K}$	w	u	y
0.1	1.125	1.066	2.73	0.385	1.82

$=\Delta c_p(T_g)$; and, i.e., both are comparable provided that $u \simeq 0.1w$, a value that we will assume in what follows thus ensuring thermodynamic consistency from the two fluctuation formulas. In summary, the existing thermodynamic measurements can determine several parameters and can allow consistent description of several thermodynamic data. Still, one free parameter, either w or y, remains since only the ratio from w to y is determined. We use this freedom to obtain the correct value of the most probable barrier at the glass temperature. Finally, we note that the above result also implies that $\frac{t_g-t_K}{t_K}=0.066$, i.e., about half of $\frac{t_A-t_K}{t_K}=0.125$. It is worth mentioning that the values of the Landau parameters are consistent with the random first-order framework as assumed. Finally, we summarize our results for the model parameters by fitting the experimentally relevant quantities to the data obtained for OTP in Table I.

APPENDIX B: DETAILS OF THE REPLICA CALCULATION FOR BARRIER FLUCTUATIONS

In this appendix we summarize the derivation of the various contributions to the barrier fluctuation given in Eq. (59). We start our calculation with the third term in Eq. (59). The other two terms are simpler to determine and can be obtained as specific limits of the third one. It holds that

$$\overline{F_{p_c,\rho_2}F_{q^*,\rho_2}} = T^2\frac{\int \mathcal{D}\rho e^{-\beta H[\rho]} \log Z_{p_c,\rho} \log Z_{q^*,\rho}}{\int \mathcal{D}\rho e^{-\beta H[\rho]}} = \lim_{m_{1,2}\to 0}(\mathcal{Y}_{12}-\mathcal{Y}_1-\mathcal{Y}_2), \tag{B1}$$

where we introduced

$$\mathcal{Y}_{12} = T^2\frac{\int \mathcal{D}\rho e^{-\beta H[\rho]} Z_{p_c,\rho}^{m_1} Z_{q^*,\rho}^{m_2} + Z}{m_1 m_2 Z},$$

$$\mathcal{Y}_1 = \frac{T^2\int \mathcal{D}\rho e^{-\beta H[\rho]} Z_{p_c,\rho}^{m_1}}{m_1 m_2 Z},$$

$$\mathcal{Y}_2 = \frac{T^2\int \mathcal{D}\rho e^{-\beta H[\rho]} Z_{q^*,\rho}^{m_2}}{m_1 m_2 \int \mathcal{D}\rho e^{-\beta H[\rho]}}, \tag{B2}$$

where $Z=\int \mathcal{D}\rho e^{-\beta H[\rho]}$. To analyze the first term in Eq. (B1) we use again the replica trick and write

$$\mathcal{I}_{12} = \lim_{m_{1,2}\to 0}\mathcal{Y}_{12} = \lim_{n,m_{1,2}\to 0}\int \mathcal{D}\varphi_1 \frac{e^{-\beta H[\varphi_1]} Z_{p_c,\rho}^{m1} Z_{q^*,\rho}^{m_2} + Z}{m_1 m_2 \left(\int \mathcal{D}\varphi e^{-\beta H[\varphi]}\right)^{n-1}} = \lim_{m_1,m_2\to 0}\lim_{n\to 0}\frac{\mathcal{I}_{p_c;q^*}^{(n;m_1,m_2)}}{m_1 m_2}. \tag{B3}$$

Here we introduced a quantity $\mathcal{I}_{p_c;q^*}^{(n;m_1,m_2)}$ that can be determined from an $n+m_1+m_2$ replicated problem with order parameter $\mathbf{Q}$,

$$\mathbf{Q} = \begin{pmatrix} r & p & q \\ p^T & u & \psi \\ q^T & \psi^T & v \end{pmatrix}. \tag{B4}$$

It holds that

$$\mathcal{I}_{p_c;q_0}^{(n;m_1,m_2)} = \int \mathcal{D}\mathbf{Q} e^{-\beta H[\mathbf{Q}]} \prod_{\mathbf{x},a}\delta[p_c(\mathbf{x})-p_{1a}(\mathbf{x})] \times \prod_{\mathbf{x},\alpha}\delta[q_0-q_{1\alpha}(\mathbf{x})]. \tag{B5}$$

$H[\mathbf{Q}]$ has the same form as Eqs. (27) and (28) if one uses the matrix $\mathbf{Q}$ of Eq. (B4) instead of the original replica variable q. The submatrices of $\mathbf{Q}$ are given as follows: r is an $n\times n$ matrix, p is an $n\times m_1$ matrix, q_0 is an $n\times m_2$ matrix, u is an $m_1\times m_1$ matrix, v is an $m_2\times m_2$ matrix, and ψ is an $m_1\times m_2$ matrix. Matrices p and q_0 obey the additional constraints,

$$p_{1b}(\mathbf{x}) = p_c(\mathbf{x}) \quad \text{for} \quad \forall\, b = 1,\ldots,m_1,$$

$$q_{1\alpha} = q_0 \quad \text{for} \quad \forall\, \alpha = 1,\ldots,m_2, \tag{B6}$$

which is enforced through the δ function above. We assume that for a replica symmetric instanton solution that and the elements of $\psi_{a\beta}$ are all the same,

$$\psi_{a\beta}(\mathbf{x}) = \psi(\mathbf{x}). \tag{B7}$$

Similarly we assume that $v_{\alpha\beta}=(1-\delta_{\alpha\beta})v$.

The analysis of $H[\mathbf{Q}]$ is tedious but straightforward and yields that it can be written as a sum of three terms,

$$H[\mathbf{Q}] = m_1\mathcal{H}_{\text{inh}}[p_c;u] + m_2\mathcal{H}_{\text{hom}}[q_0;v] + m_1 m_2\mathcal{V}[\psi]. \tag{B8}$$

Here

$$\mathcal{H}_{\text{hom}}[q^*;v] = \int d^3\mathbf{x}\left\{2h[q^*] + (m_2-1)h[v] - (m_2-1)vq^{*2} - \frac{1}{3}(m_2-1)v^3\right\}$$

refers to the homogeneous problem. In addition,

$$\mathcal{H}_{\text{inh}}[p_c;u] = \int d^3\mathbf{x}\Big\{ 2h[p_c] + (m_1-1)h[u] - (m_1-1)u(\mathbf{x})p_c^2(\mathbf{x}) - \frac{1}{3}(m_1-1)(m_1-2)u^3(\mathbf{x})\Big\}$$

is the contribution of the inhomogeneous instanton. Finally, the coupling term between the two is given as

$$\mathcal{V}[\psi] = \int d^3\mathbf{x}\{2h[\psi] + [(m_1-1)u_0(\mathbf{x}) + (m_2-1)v]\psi^2(\mathbf{x}) - 2p_c(\mathbf{x})q^*\psi(\mathbf{x})\}.$$

In order to determine the various matrix elements of $\mathbf{Q}$ defined in Eq. (B4) we perform saddle-point approximations with respect to the numerous variables. We find $u(\mathbf{x})=r(\mathbf{x})$ which has been calculated earlier. Similarly it follows that $v=q^*$. The saddle-point equation for ψ is then

$$p_c(\mathbf{x})q_0 = -\nabla^2\psi(\mathbf{x}) + t\psi(\mathbf{x}) - \alpha\psi^2(\mathbf{x}) + y\psi^3(\mathbf{x}) + [r_0(\mathbf{x}) + q^*]\psi(\mathbf{x}), \tag{B9}$$

and it follows that the solution of this equation is $\psi(\mathbf{x})=p_c(\mathbf{x})$. With these results we are in the position to calculate the barrier fluctuations.

First we rewrite expression (B1) by employing the saddle-point solution as follows:

$$\overline{F_{p_c,\rho_2}F_{q^*,\rho_2}} = \lim_{m_{1,2}\to 0}\frac{1}{m_1m_2}(1 - e^{-m_2\beta\mathcal{H}_{\text{hom}}[q^*,q^*]} - e^{-m_1\beta\mathcal{H}_{\text{inh}}[p_c;r_0,r_1]} + e^{-m_1\beta\mathcal{H}_{\text{inh}}[p_c;r_0,r_1]-m_2\beta\mathcal{H}_{\text{hom}}[q^*,q^*]-m_1m_2\beta\mathcal{V}[p_c]}). \tag{B10}$$

Expanding the exponents up to the second order in m_i's and taking $r_{0,1}=p_c$ yield expression (57) in the text. Equation (55) can be obtained using the same steps which lead us to Eq. (B10). For example, we have

$$\overline{F^2_{p_c,\rho_2}} = \lim_{m_{1,2}\to 0}\frac{1}{m_1m_2}(1 - e^{-m_2\beta\mathcal{H}_{\text{inh}}[p_c;r_0,r_1]} - e^{-m_1\beta\mathcal{H}_{\text{inh}}[p_c;r_0,r_1]} + e^{-(m_1+m_2)\beta\mathcal{H}_{\text{inh}}[p_c;r_0,r_1]-m_1m_2\beta\mathcal{V}_{\text{inh}}[p_c]}), \tag{B11}$$

where we introduced $\mathcal{V}_{\text{inh}}[p_c]=\int d^3\mathbf{x}h[p_c]$. Upon taking the limit $m_{1,2}\to 0$ and using the replica symmetry $r_0=r_1=p_c$ we recover the second expression in Eq. (59)

APPENDIX C: EXPRESSION FOR THE INTEGRATION CONSTANT z_0

In this section we provide an expression for the integration constant z_0 which enters into Eq. (53) for the interface profile. First, we define the following functions:

$$q_0(t) = \frac{w}{2y}\left(1 + \sqrt{1 - \frac{8t}{9t_K}}\right), \quad \tilde{t} = \frac{3}{2}t_K - t,$$

$$q_m(t) = \sqrt{\frac{y}{\tilde{t}}}\left[q_0(t) - \frac{w}{3y}\right], \quad \varphi(t) = \sqrt{\frac{3q_m^2(t)-1}{2}}. \tag{C1}$$

In terms of these functions the expression for $z_0(t)$ reads as

$$z_0(t) = \frac{1}{4}\log\left[\frac{q_m(t)+\varphi(t)}{q_m(t)-\varphi(t)}\right]. \tag{C2}$$

Finally, we remark that the integral, which determines the length scale $\rho(t)$ [Eq. (66)] can be computed exactly using relations above. The resulting expression is quite cumbersome and will not be listed here.

[1] K. Schmidt-Rohr and H. W. Spiess, Phys. Rev. Lett. **66**, 3020 (1991); U. Tracht, M. Wilhelm, A. Heuer, H. Feng, K. Schmidt-Rohr, and H. W. Spiess, *ibid.* **81**, 2727 (1998).
[2] E. V. Russell and N. E. Israeloff, Nature (London) **408**, 695 (2000).
[3] R. Richert, J. Phys.: Condens. Matter **14**, R703 (2002).
[4] W. Götze, in *Liquids, Freezing and Glass Transition*, edited by J.-P. Hansen, D. Levesque, and J. Zinn-Justin (North-Holland, Amsterdam, 1991), p. 287.
[5] T. R. Kirkpatrick and P. G. Wolynes, Phys. Rev. A **35**, 3072 (1987).
[6] T. R. Kirkpatrick and D. Thirumalai, Phys. Rev. Lett. **58**, 2091 (1987).
[7] R. Richert and C. A. Angell, J. Chem. Phys. **108**, 9016 (1998).
[8] T. R. Kirkpatrick, D. Thirumalai, and P. G. Wolynes, Phys. Rev. A **40**, 1045 (1989).
[9] M. Mezard and G. Parisi, J. Phys.: Condens. Matter **12**, 6655 (2000).
[10] J.-P. Bouchaud and G. Biroli, J. Chem. Phys. **121**, 7347 (2004).
[11] X. Xia and P. G. Wolynes, Proc. Natl. Acad. Sci. U.S.A. **97**, 2990 (2000).
[12] X. Xia and P. G. Wolynes, Phys. Rev. Lett. **86**, 5526 (2001).
[13] V. Lubchenko and P. G. Wolynes, Phys. Rev. Lett. **87**, 195901 (2001).
[14] V. Lubchenko and P. G. Wolynes, J. Chem. Phys. **121**, 2852 (2004).
[15] G. Adam and J. H. Gibbs, J. Chem. Phys. **43**, 139 (1965).
[16] S. Capaccioli, G. Ruocco, and F. Zamponi, J. Phys. Chem. B **112**, 10652 (2008).
[17] M. E. Cates and S. Ramaswamy, Phys. Rev. Lett. **96**, 135701 (2006).
[18] S. Franz and G. Parisi, J. Phys. I **5**, 1401 (1995).
[19] S. Franz, J. Stat. Mech.: Theory Exp. (2005) P04001.
[20] M. Dzero, J. Schmalian, and P. G. Wolynes, Phys. Rev. B **72**, 100201(R) (2005).
[21] G. Diezemann, Europhys. Lett. **53**, 604 (2001).
[22] L. F. Cugliandolo and J. L. Iguain, Phys. Rev. Lett. **85**, 3448 (2000).
[23] F. Fujara, B. Geil, H. Sillescu, and G. Fleischer, Z. Phys. B: Condens. Matter **88**, 195 (1992).

[24] M. T. Cicerone and M. D. Ediger, J. Chem. Phys. **104**, 7210 (1996).
[25] Y. Singh, J. P. Stoessel, and P. G. Wolynes, Phys. Rev. Lett. **54**, 1059 (1985).
[26] T. V. Ramakrishnan and M. Yussouff, Phys. Rev. B **19**, 2775 (1979).
[27] C. H. Bennett, J. Appl. Phys. **43**, 2727 (1972).
[28] R. Monasson, Phys. Rev. Lett. **75**, 2847 (1995).
[29] M. Mezard and G. Parisi, Phys. Rev. Lett. **82**, 747 (1999).
[30] J. P. Stoessel and P. G. Wolynes, J. Chem. Phys. **80**, 4502 (1984).
[31] Th. M. Nieuwenhuizen, Phys. Rev. Lett. **80**, 5580 (1998).
[32] H. Westfahl, Jr., J. Schmalian, and P. G. Wolynes, Phys. Rev. B **68**, 134203 (2003).
[33] L. F. Cugliandolo and J. Kurchan, Phys. Rev. Lett. **71**, 173 (1993).
[34] L. D. Landau and E. M. Lifshitz, *Statistical Physics* (Pergamon, London, 1980).
[35] E. Donth, J. Non-Cryst. Solids **53**, 325 (1982).
[36] S. Wu, J. Schmalian, G. Kotliar, and P. G. Wolynes, Phys. Rev. B **70**, 024207 (2004).
[37] J.-P. Bouchaud, L. Cugliandolo, J. Kurchan, and M. Mézard, Physica A **226**, 243 (1996).
[38] H. Westfahl, Jr., J. Schmalian, and P. G. Wolynes, Phys. Rev. B **64**, 174203 (2001).
[39] S. Franz and G. Parisi, Phys. Rev. Lett. **79**, 2486 (1997).
[40] D. J. Gross, I. Kanter, and H. Sompolinsky, Phys. Rev. Lett. **55**, 304 (1985).
[41] X. H. Qiu and M. D. Ediger, J. Phys. Chem. B **107**, 459 (2003).
[42] M. Tarzia and M. A. Moore, Phys. Rev. E **75**, 031502 (2007).
[43] A. Barrat, S. Franz, and G. Parisi, J. Phys. A **30**, 5593 (1997).
[44] See the appendix of G. Parisi, G. Ruocco, and F. Zamponi, Phys. Rev. E **69**, 061505 (2004) for a transparent discussion of this issue.
[45] J. R. L. de Almeida and D. J. Thouless, J. Phys. A **11**, 983 (1978).
[46] G. Cwilich and T. R. Kirkpatrick, J. Phys. A **22**, 4971 (1989).
[47] A. Crisanti and H.-J. Sommers, Z. Phys. B: Condens. Matter **87**, 341 (1992).
[48] S. Franz and A. Montanari, J. Phys. A: Math. Theor. **40**, F251 (2007).
[49] J. S. Langer, Ann. Phys. **41**, 108 (1967).
[50] S. Franz, Europhys. Lett. **73**, 492 (2006).
[51] M. A. Moore, Phys. Rev. Lett. **96**, 137202 (2006); M. A. Moore and J. Yeo, *ibid.* **96**, 095701 (2006).
[52] K. H. Fischer and J. A. Hertz, *Spin Glasses*, Cambridge Studies in Magnetism (Cambridge University Press, London, 1991).
[53] Ch. Unger and W. Klein, Phys. Rev. B **29**, 2698 (1984).
[54] G. Biroli, J.-P. Bouchaud, A. Cavagna, T. S. Grigera, and P. Verrocchio, arXiv:0805.4427 (unpublished).
[55] S. D. Gottke, D. D. Brace, G. Hinze, and D. Fayer, J. Phys. Chem. B **105**, 238 (2001).
[56] R. J. Greet and D. Turnbull, J. Chem. Phys. **47**, 261 (1970).
[57] S. S. Chang and A. B. Bestul, J. Chem. Phys. **56**, 503 (1972).
[58] R. J. Greet and D. Turnbull, J. Chem. Phys. **46**, 1243 (1967).
[59] G. P. Johari, J. Chem. Phys. **112**, 8958 (2000).
[60] L.-M. Wang, V. Velikov, and C. A. Angell, J. Chem. Phys. **117**, 10184 (2002).
[61] J. T. Edward, J. Chem. Educ. **47**, 261 (1970).